Supporting Information

Butch et al. 10.1073/pnas.1120273109

SI Text

Scaling of the Quadratic Coefficient A_2 of the Resistivity in the Fermi Liquid State. Fits to the electrical resistivity of the form $\rho = \rho_0 + A_2 T^2$ were performed on the high field side of B_c, i.e., in the field-induced Fermi liquid (FL) ground state. As a function of magnetic field, the data scale with identical critical exponent $\alpha = 0.38$. This analysis was performed on data from multiple samples at each concentration. In order to plot the data together in Fig. 4*A*, the absolute values of the coefficients for each sample were scaled by a constant value, which maintains the integrity of the scaling analysis. The necessity for rescaling is expected because of the sensitivity of the scattering to sample dependence beyond experimental control, which makes the success of the A_2 scaling all the more remarkable. A similar approach was used to put together Fig. 4*B*. Note that, experimentally, the step size is much coarser in the doping direction, and the uncertainty is larger due to the aforementioned sample dependence.

Resistivity Scaling Above the Fermi Liquid Boundary B_c. The scaling of $\rho(T)$ reflects the fact that the resistivity $\Delta\rho$ can be described generally as a function $A_2 T^2 f(\Delta B^\gamma/T)$, where $\Delta B = B - B_c$, that is applicable to scattering in both Fermi liquid ($\Delta\rho \propto T^2$) and non-Fermi liquid (NFL) ($\Delta\rho \propto T^n$) regions. In this framework, the T^n behavior in the NFL region stems from anomalous temperature dependence in A_2, which is by definition a constant in temperature in the FL state. The resultant picture is that T_{FL} separates the FL state at high magnetic field and low temperature from the NFL region at low magnetic field and high temperature, consistent with the magnetic field dependence of T_{FL} (Fig. 1*C*). This picture also suggests that upon crossing T_{FL} the dominant energy scale is transferred from temperature to magnetic field, which implicitly suggests that any dominant energy scale, such as Fermi energy, is absent.

The exponents α, γ, and n are related as $\alpha = \gamma(2 - n)$ by considering the following asymptotic limits: (*i*) Fermi liquid ($T \ll \Delta B$): $\Delta\rho = A_2(B)T^2$. In this limit, $\Delta\rho/A_2(B)T^2 = 1$ and thus $f(\Delta B^\gamma/T) \to 1$. (*ii*) Non-Fermi liquid ($T \gg \Delta B$):$\Delta\rho = A_n T^n = A_2(B)T^2 \times (\Delta B^\gamma/T)^{2-n}$. Our data show that when $n < 2$, $\Delta\rho < A_2(B)T^2$ and thus $f(\Delta B^\gamma/T) < 1$. Note that it is possible to define $A_2'(B, T) = A_2(B) \times (\Delta B^\gamma/T)^{2-n}$, or in other words, explicitly add a temperature dependence to A_2, which is a constant in temperature in the Fermi liquid state. However, from Fig. 4*A* we already know that $A_2 \propto \Delta B^\alpha$, and because A_2 and $A_2{}'$ must have the same magnetic field dependence, it follows that $\gamma(2 - n) = \alpha$.

For $x = 0.17$, scaling is satisfied using an exponent $\gamma = 1.0 \pm 0.02$, so $\alpha = 0.38$ forces $n \approx 1.6$. For $x = 0.15$, scaling is satisfied using an exponent $\gamma = 0.4 \pm 0.1$, so $\alpha = 0.38$ forces $n \approx 1.0$ (Fig. S4).

The plots in Fig. 4 show the difference between Fermi liquid and non-Fermi liquid behavior. In the Fermi liquid state, $\Delta\rho/A_2T^2 = 1$ by definition, and the slope of the scaled curve is zero. In contrast, in the non-Fermi liquid regime the slope of the scaled curve is positive, reflecting the notion that A_2 is no longer a constant.

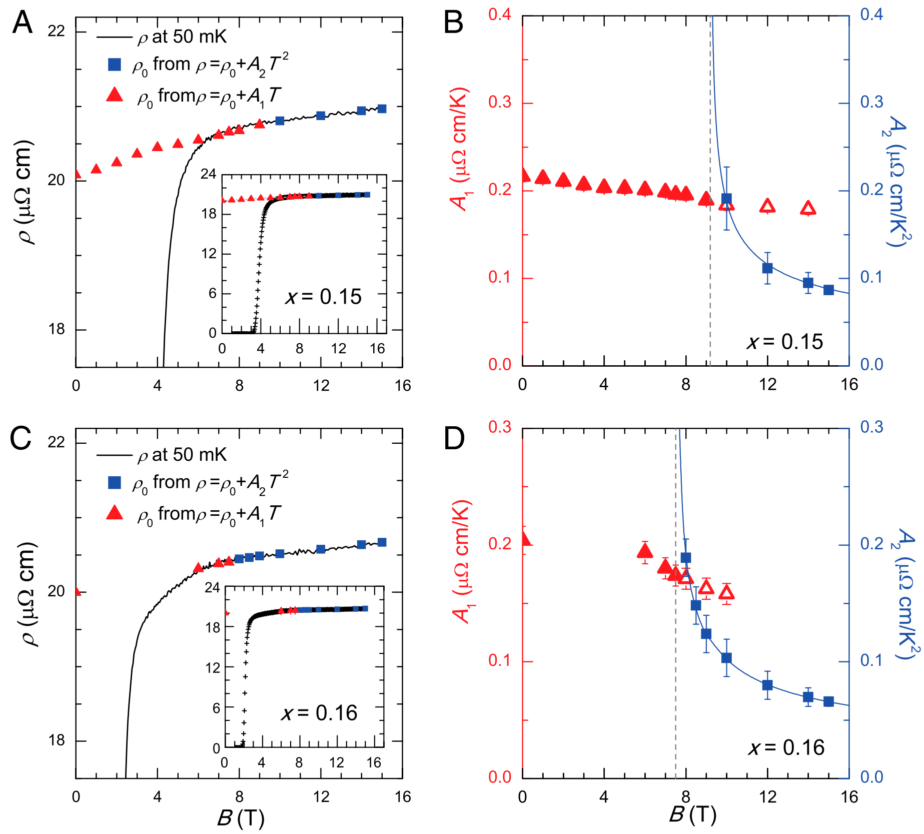

Fig. S1. Magnetic field dependence of resistivity ρ in the low temperature limit. *A* and *C* present vertical zooms of magnetoresistance data measured at a constant temperature of 50 mK for $x = 0.15$ and $x = 0.16$, respectively, and the residual ($T = 0$) resistivity ρ_0 obtained from extrapolated fits of $\rho(T)$ at different constant fields. Insets present the full vertical axis scales for each dataset. *B* and *D* present the field dependence of inelastic scattering coefficients A_1 (red) and A_2 (blue) for $x = 0.15$ and $x = 0.16$, respectively, demonstrating the persistence of finite-temperature $\Delta\rho \propto T$ scattering beyond the critical field (dashed line), which is the critical boundary of $\Delta\rho \propto T$ and $\Delta\rho \propto T^2$ regions at zero temperature. Note that although A_2 exhibits an upturn at the critical field, A_1 is completely insensitive to B_c.

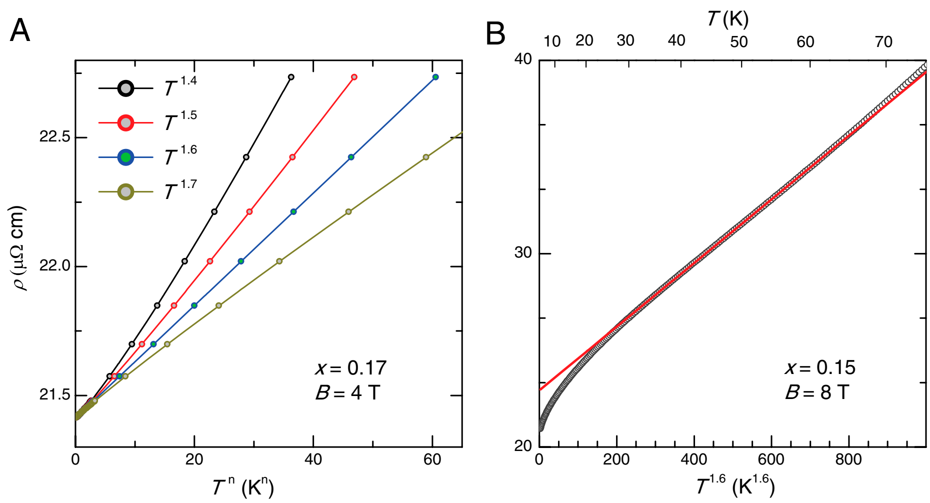

Fig. S2. Determination of $T^{1.6}$ resistivity. (*A*) Comparison of different power law temperature fits of the resistivity for $x = 0.17$ in a magnetic field of 4 T, where both $\Delta\rho \propto T$ and $\Delta\rho \propto T^2$ behaviors vanish. It is clear that a $T^{1.6}$ power yields the best fit, as shown by the blue data. (*B*) Demonstration of the range of the approximate $T^{1.6}$ power law fit for $x = 0.15$ in a field of 8 T, where $\Delta\rho \propto T$ behavior is dominant from zero temperature up to a cross-over temperature of approximately 20 K where the approximate $T^{1.6}$ power law becomes dominant and then extends up to approximately 60 K.

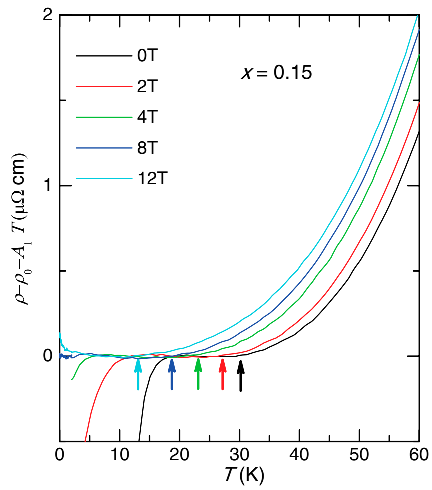

Fig. S3. Residuals of linear fits for $x = 0.15$. The definition of T_1 is denoted by arrows. Of particular note are the 8 T data (blue line) where temperature-linear resistivity extends from 20 mK up to approximately 20 K.

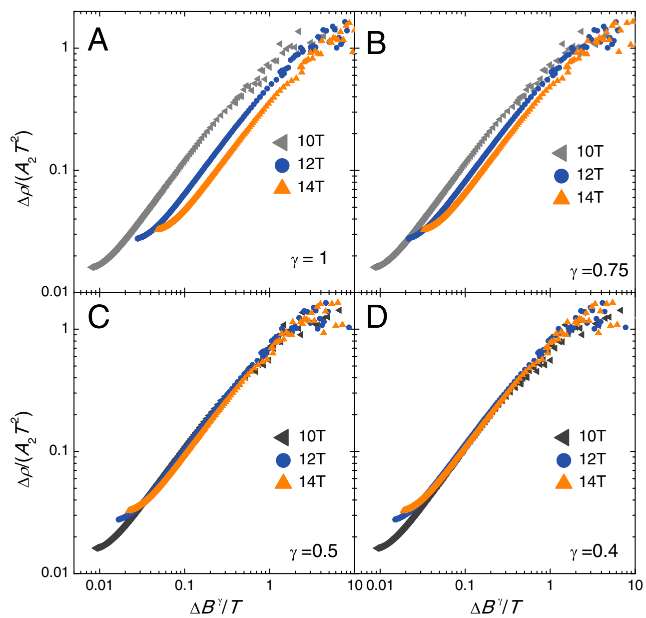

Fig. S4. Determination of resistivity scaling for $x = 0.15$. This series of plots demonstrates that γ should be considered as an independent fitting parameter and that the success of the scaling and its agreement with the critical scaling of A_2 as a function of B is a demonstration of self-consistency between the exponents. For instance, it is clear in *A* that the scaling exponent for $x = 0.15$ is not 1.0 (i.e., in contrast to the scaling observed for $x = 0.17$ with a choice of $\gamma = 1.0$, as shown in Fig. 4*D*).